Automatic Parallel Parking in Tiny Spots: Path Planning and Control

Hélène Vorobieva, Sébastien Glaser, Nicoleta Minoiu-Enache, and Saïd Mammar, *Senior Member, IEEE*

***Abstract*—This paper presents automatic parallel parking for a passenger vehicle, with highlights on a path-planning method and on experimental results. The path-planning method consists of two parts. First, the kinematic model of the vehicle, with corresponding geometry, is used to create a path to park the vehicle in one or more maneuvers if the spot is very narrow. This path is constituted of circle arcs. Second, this path is transformed into a continuous-curvature path using clothoid curves. To execute the generated path, control inputs for steering angle and longitudinal velocity depending on the traveled distance are generated. Therefore, the traveled distance and the vehicle pose during a parking maneuver are estimated. Finally, the parking performance is tested on a prototype vehicle.**

***Index Terms*—Intelligent vehicles, motion control, motion planning, path planning.**

I. Introduction

NOWADAYS, the rare vacant parking spots have become very narrow in big cities. Drivers cannot afford to search bigger spots and have to be very attentive when maneuvering their vehicles. Even for experienced drivers, this often leads to minor scratches on their cars. Moreover, several repositioning maneuvers can increase traffic jams. Consequently, such parking might be damaging for a car and stressful for a driver. Therefore, automatic parking is a solution to increase drivers' comfort and security. Furthermore, with multiple repositioning being eliminated, the maneuver would be faster, which would improve the circulation and reduce the stress of all road users. Fully automatic parking gives a driver the choice to let his vehicle park itself even if the driver is not inside the car, thus saving time. Such parking can also be used in the context of autonomous parking valet, with autonomous driving of the vehicle from a parking spot to a pickup point and from a deposit point to the parking spot.

Manuscript received March 7, 2014; revised June 16, 2014; accepted June 19, 2014. The Associate Editor for this paper was M. Da Lio.

H. Vorobieva is with University of Évry Val d'Essonne, 91025 Évry, France, and also with Renault SAS, 78084 Guyancourt, France (e-mail: helene.vorobieva@renault.com).

S. Glaser is with Laboratoire sur les Interactions Véhicules-Infrastructure-Conducteurs, Institut Français des Sciences et Technologies des Transports, de l'Aménagement et des Réseaux, 78000 Versailles, France (e-mail: sebastien.glaser@ifsttar.fr).

N. Minoiu-Enache is with Renault SAS, 78084 Guyancourt, France (e-mail: nicoleta.minoiu-enache@renault.com).

S. Mammar is with Laboratoire Informatique, Biologie Intègrative et Systémes Complexes, University of Évry Val d'Essonne, 91025 Évry, France (e-mail: said.mammar@ibisc.univ-evry.fr).

Color versions of one or more of the figures in this paper are available online at http://ieeexplore.ieee.org.

Digital Object Identifier 10.1109/TITS.2014.2335054

Putting legal aspects aside, to be commercialized, automatic parking has to be fast, predictable, and not very demanding for the tires. Low computational time and few sensors are additional constraints for such an assistance system.

A. State of the Art

There are several methods to generate the trajectory for the parallel parking problem.

Methods based on the use of reference functions are implemented in [1] and [2]. In [1], a method using the Lyapunov function is presented to stabilize the vehicle in the parking spot. In [2], an optimization of two parameters is proposed to find the steering angles and the duration of commands to execute the parking maneuvers. These methods strongly depend on gains and parameters chosen for the functions, which can be difficult to adjust and do not ultimately lead to correct parking maneuvers.

Methods based on fuzzy logic or neural networking to learn a human technique are implemented in [3] and [4]. Some methods provide reference trajectories, e.g., in [5] and [6], or provide only the commands in function of the pose of the vehicle at each step, e.g., in [7] and [8]. Although those methods can be effective solutions to deal with uncertainties and inaccuracies in the mapping of the environment, they can be limited to human experts' knowledge (for the learning step) or may need a relatively long parking space to park a car [3]. Those methods are also difficult to generalize.

Methods using a potential field or a direction field are introduced in [9] and [10]. These methods can be applied to all parking configurations; nevertheless, the generation of a solution needs much computation time, the convergence is not guaranteed in complex situations, and the solution strongly depends on the optimization parameters.

Methods based on two path-planning phases consist of creating a collision-free path by a lower level geometric planner that ignores the motion constraints [11], [12]. Then, this path is subdivided to create an admissible path. An optimization routine can reduce its length. Very often, these methods present continuous-curvature paths, e.g., in [13], where a clothoidal curve is used. These methods can effectively solve the problems of collision avoidance and nonholonomic constraints of the parking control. However, these methods are more adapted to general path planning and become very complicated when applied to the parking problem, e.g., with a generation of a lot of forward or backward maneuvers sets. Recently, in [14], a segmental path-planning method based on a two-step approach for initial entering into parking has been presented. As the

back-and-forth shuttling maneuvers are done using a geometric predictable method, this path planning is less complex than the other methods. Nevertheless, initial entering has to be optimized and consequently requires complex computational resources as all two-path-planning-phase methods do, which can be undesirable in industrial context.

The geometric methods based on admissible circular arcs use trajectories with easy geometrical equations. Some methods have been presented for parking in one maneuver only, as in [15], where the path is composed of two circle arcs, and these can be found for any initial pose if the spot is long enough or, as in [16], with a trajectory defined by two circle arcs linked by a straight line. Other methods allow parking in several maneuvers, e.g., in [17], where a forbidden zone is defined and the car can park by traveling outside it with a path formed by circle arcs. An interesting approach in parking in one maneuver that is based on retrieving a vehicle from a parking spot and then reversing this procedure was proposed in [18] and [19]. In this method, the initial orientation of the vehicle has to be parallel to the parking spot. Whereas the length of the minimum parking spot depends on the initial position of the vehicle in the method proposed in [15], the minimal length proposed in the reversed method in [18] and [19] depends only on the characteristics of the vehicle.

As the reversed geometric approach is particularly close to the human approach and adapted to the parking problem in an industrial context by its simplicity, in a recent work [20], we have extended this method to parking in several trials, with any initial position and orientation of the vehicle, for spots that are just longer than the length of the vehicle. As such a geometric method implies steering at stop, which can wear the tires and heat the electric power steering, we extended it to continuous-curvature path planning with clothoidal curves in [21]. Recently, as shown in [22], we have tested this method by experimenting on a real vehicle.

B. Contribution and Content of This Paper

In this paper, we first detail the functional architecture of automatic parking introduced in [22]. Then, we thoroughly present all the steps that lead to automatic parking, from the trajectory generation (introduced in [20] and [21]) to the execution of the maneuver on a real prototype (as in [22]).

In addition to the novelty of the presentation of a full system, new parking strategies and feasibility discussions are added. Comparisons of different methods are also provided.

More specifically, the automatic parking approach presented in [22] is enlarged with conditions for the end of the parking, which can occur at any time that the vehicle stops. The emergency stop is also taken into account.

The feasibility of the parking maneuver is carefully studied, enlightening the conditions for the execution of the first circle arc of entrance in the parking. A new study on the minimal width of the parking spot is also provided, introducing the differences between parking near a wall and parking on a place without obstacle at the lateral side.

An extension of the geometric reversed parking for parallel parking beginning with a forward maneuver is presented. Its advantages and disadvantages are presented with respect to the classic backward parking.

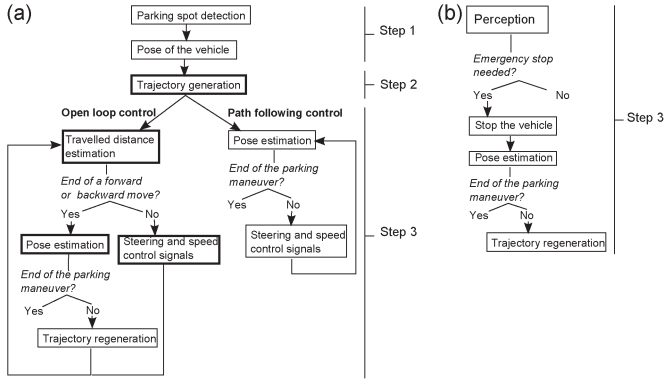

Fig. 1. Approach for automatic parking. (a) Parts of the parking routine. (b) Emergency stop routine, which can occur at any moment during step 3.

A detailed comparison of the different geometric path planning methods is carried out, and the differences introduced by the continuous-curvature path planning are discussed. All numerical applications presented for this purpose are done with the size parameters of the vehicle used for the experiments.

In the succeeding section, the approach for automatic parallel parking is presented. Section III details the methods for the geometric path planning. In Section IV, we explain the continuous-curvature path-planning extension. Then, Section V is dedicated to a discussion of the different path-planning methods. In Section VI, the control signals and the pose estimation are outlined. Experimental results for the steering, acceleration, brake actuators, and the parking maneuver are presented in the Section VII. Section VIII wraps up this paper and summarizes the main items.

II. Approach of Automatic Parking

A. Functions of Automatic Parking

Automatic parking can be divided into three parts: perception, path planning, and execution of the maneuvers (see Fig. 1).

The first function, i.e., perception, consists of detecting the size and position of the parking spot and estimating the pose of the vehicle compared with this spot. A common solution is to make the vehicle travel next to the spot and scan the spot for its length and width (e.g., with ultrasonic sensors [23]). Another solution is to detect the parking spot by image processing using cameras attached to four sides of the vehicle [24]. Consequently, the pose of the vehicle is deduced with respect to the parking spot. Intelligent infrastructures can also be considered to detect the pose of the vehicle in the parking spot and, more generally, to communicate the location of the free spots to the vehicle.

The second function of the parking approach is to calculate the trajectory needed to enter the parking spot. The result of this path generation can be the exact coordinates of the path in a reference system or another set of information sufficient to park the vehicle.

The final function makes two parallel routines intervene: the execution of the maneuvers and the routine of the emergency

stop. At each moment, if an emergency stop is needed, the execution of the maneuvers is paused. In this case, the emergency routine sends a zero speed request to the vehicle. Such a stop can be needed, for example, if the distance to the obstacle is too short (depending on the precision of the sensors) or if the intelligent infrastructure or the driver orders a stop. Once the vehicle is stopped, if there is no danger and if the vehicle is not yet well parked, the maneuvers can be started again, with an eventual path regeneration.

The execution of the maneuvers can be performed by two different control strategies.

- *Path following control:* The control signals for the actuators are adjusted to the pose estimation at each time step. This solution requires good pose estimation and therefore precise exteroceptive sensors. Such control strategies are mostly used for long trajectories with high longitudinal speed. This solution can be considered if the coordinates of the points on the path can be easily calculated. Consequently, this approach is not entirely appropriate for a parking system with minimum sensor equipment.
- *Open-loop control with optional trajectory regeneration:* In this approach, the control signals are deduced from the trajectory and depend only on the traveled distance. This precalculated distance can be estimated using internal sensors of the vehicle. To have a more precise parking maneuver, trajectory regeneration can be carried out to close the position control loop. For example, each time the vehicle stops, the trajectory is recalculated based on the pose estimation from internal or exteroceptive sensors. In a low-cost solution, the initial pose of the vehicle and the parking spot could be less precise; here, the trajectory regeneration helps in reducing path-tracking errors. This solution is also easier to implement if the signals can be deduced without calculating the coordinates of the points on the path. It should be noted that, in this strategy, the emergency stop is more critical as it has to minimize the impact of the drift of the sensors.

During the execution of the maneuvers, an additional decision algorithm can be used each time the vehicle stops. A set of criteria $C1$ is defined so that, if the pose of the vehicle satisfies $C1$, then this pose is good enough to be the final pose of the vehicle and the parking routine is stopped (even if all the planned maneuvers have not been executed). If a passenger or a remote operator is present, a second set $C2$ of criteria for a correct parking pose, but more permissive than $C1$, can be added. If the pose of the vehicle satisfies $C2$ but not $C1$, the passenger or the remote operator could decide to continue or not with the maneuvers.

B. Sensors and Perception

Modern cars are equipped with antilock braking system (ABS) that utilizes angular encoders measuring the speed of the four wheels. The steering wheel angle is also commonly available. Consequently, these internal measurements can be used for all systems, independent of the specific sensors that can be added on the vehicle and that might increase the price and the complexity of the automatic parking feature. Some exteroceptive sensors are also often added to help the driver: ultrasound sensors, telemeters, or cameras. Even if the provided information is not always very accurate, the perception can be achieved using low-cost sensors. The information from these sensors should permit to model the environment, to detect the parking spot, and to localize the vehicle as it is done in hands-free parking devices. An autonomous navigation can also be added in semi-controlled environments with infrastructure sensors [25].

C. Actuators

Different actuators and associated calculators needed to pilot a vehicle exist already in the vehicles, but they might need supplementary software modifications. The steering is automatically performed through the steering column with an electronic power steering calculator, the acceleration is provided by the engine with the engine control unit, and the braking comes from the braking system with the electronic stability program (ESP)/ABS calculator.

D. Our Contribution in the Parking Approach

This paper concerns the second part with the path-planning section and some subparts of the third part in the open-loop control approach (bold boxes in Fig. 1). We present also the control of the steering signal. Moreover, the distance and the pose estimation are performed by using only internal vehicle sensors. The experimental results exemplify the treated aspects of the parking maneuver.

III. Geometric Parking

A. Parking in One Maneuver

1) Preliminary Definitions: The parking maneuver is a low-speed movement. Consequently, the Ackerman steering is considered with the four wheels rolling without slipping, around the instantaneous center of rotation (ICR) C_l and C_r for, respectively, left and right steering. Different turning radii are calculated. With E being the center of the rear track

$$R_E = \frac{a}{\tan\delta}. \tag{1}$$

The other radius can be deduced geometrically. The radius from the points situated on the longitudinal axis of symmetry of the vehicle do not differ with right or left steering, e.g., $R_E = R_{El} = R_{Er}$. However, this radius differs for the other points, and in that case, the direction of the steering is clarified as

$$\begin{aligned} R_{Bl} &= \sqrt{(R_E + b + d_r)^2 + (a + d_{\text{front}})^2} \\ R_{Br} &= \sqrt{(R_E - b - d_r)^2 + (a + d_{\text{front}})^2} \\ R_{Al} &= \sqrt{(R_E + b + d_r)^2 + d_{\text{rear}}^2}. \end{aligned} \tag{2}$$

We approximate the maximum right and left steering angles to be equal and associate the different minimum radii, e.g., $R_{E\min}$ or $R_{Bl\min}$. The notations used for the vehicle are

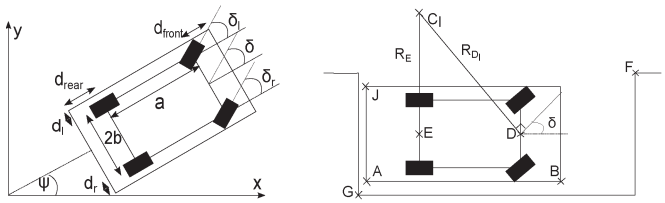

Fig. 2. Vehicle in (left) global (x, y, ψ)-coordinates and in (right) a parking spot.

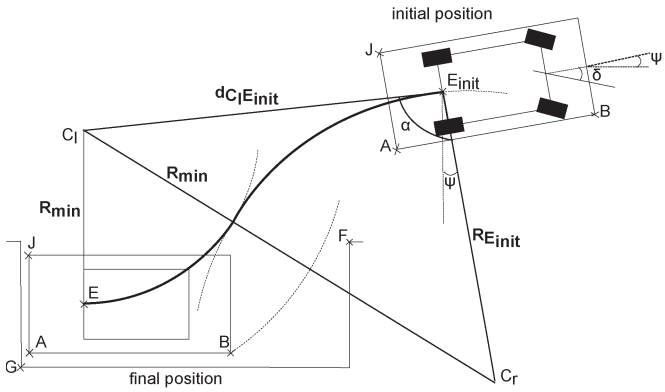

Fig. 3. Strategy for parallel parking in one trial.

presented in Fig. 2. We also denote $\mathcal{C}(C,\ R)$ as a circle of center C and of radius R, and $R_{\min} = R_{E\min}$.

2) Strategy: To park the vehicle in one trial, the problem is taken in the reversed way by retrieving the vehicle from the parking spot. A trial or a maneuver is defined as a sequence without velocity sign changes. It is assumed that the parking spot is long enough for one trial parking and that the distance between the rear vehicle and the parking vehicle, at the end of the parking maneuver, is small. In these conditions, to exit the parking spot, a human driver steers the front wheels to the maximum angle toward the outside of the parking spot and moves forward until the vehicle is retrieved. After that, the driver steers to the opposite side to drive into the road. This creates a path in two circle arcs, connected by a tangential point. This type of trajectory supposes that the steering is done at a complete stop of the vehicle.

To obtain a minimum length path, in [19], taking both circles of minimum radius is proposed. Moreover, the initial pose of the car has to be parallel to the parking spot. This means that, at the beginning of the maneuver, the car has to be perfectly positioned and parallel to the parking spot. In [20], we propose to allow any initial position and orientation for the vehicle (see Fig. 3). This creates a path with a first circle arc of radius greater or equal to the minimum radius. One of the advantages is less steering at stop. Furthermore, this gives the possibility to calculate a new maneuver at any moment without replacing the vehicle at the initial position, for instance, if the performed path of the vehicle differs from the calculated one.

In the sequel, we present the method to create such a path. The first arc of the circle for retrieving (which is the second in the parking maneuver) is of minimum radius, but the second has to connect the first circle with the real initial position of the car. As the first arc of the circle is of minimum radius and as the spot where the car has to park is known, the coordinates of C_l can be deduced. During this arc of the circle, the point E goes all over $\mathcal{C}(C_l,\ R_{\min})$. For the second arc of the circle, we search $\mathcal{C}(C_r,\ R_{E_{\text{init}}})$, which allows E to go from the initial vehicle position to $\mathcal{C}(C_l,\ R_{\min})$. By applying the Al-Kashi theorem to the triangle $E_{\text{init}}C_rC_l$ (see Fig. 3), it yields

$$R_{E_{\text{init}}} = \frac{d^2_{C_l E_{\text{init}}} - R^2_{\min}}{2R_{\min} + 2d_{E_{\text{init}}C_l}\cos\alpha} \tag{3}$$

with $\alpha = \psi + \arccos((y_{E_{\text{init}}} - y_{C_l})/d_{E_{\text{init}}C_l})$. The steering angle is then deduced as follows: $\delta = \arctan(a/R_{E_{\text{init}}})$.

3) Feasibility of the First Circle Arc: One condition for the feasibility of the presented parking maneuver is the admissibility of the first circle arc $\mathcal{C}(C_r,\ R_{E_{\text{init}}})$. It is admissible if $R_{E_{\text{init}}} \geq R_{\min}$ as the vehicle can execute any steering smaller than the possible maximum. Moreover, as we want the vehicle parked in a backward move, another condition is $x_{E_{\text{init}}} \geq x_{C_l}$. If these conditions are not satisfied, the vehicle has to go forward or backward without steering from its initial position E_{init} until it arrives to a point E_{correct} satisfying the two conditions. The coordinates of E_{correct} can be calculated by applying the Al-Kashi theorem to the triangle $C_lC_rE_{\text{correct}}$ and taking the minimal condition $R_{E_{\text{correct}}} = R_{\min}$ as

$$3R^2_{\min} - d^2_{C_l E_{\text{correct}}} + 2d_{C_l E_{\text{correct}}} R_{\min}\cos\alpha = 0 \tag{4}$$

with

$$\begin{cases} d_{C_l E_{\text{correct}}} = \sqrt{(x_{Cl} - x_{E_{\text{correct}}})^2 + (y_{Cl} - y_{E_{\text{correct}}})^2} \\ \alpha = \arccos\frac{y_{E_{\text{correct}}} - y_{Cl}}{d_{C_l E_{\text{correct}}}} + \psi_{E_{\text{init}}} \\ y_{E_{\text{correct}}} = y_{E_{\text{init}}} - (x_{E_{\text{init}}} - x_{E_{\text{correct}}})\tan\psi_{E_{\text{init}}}. \end{cases} \tag{5}$$

The resolution of (4) leads to a second-order equation for $x_{E_{\text{correct}}}$ with one solution satisfying $x_{E_{\text{init}}} \geq x_{C_l}$. The coordinate $y_{E_{\text{correct}}}$ is then deduced. There are some configurations of initial pose of the vehicle when no solution can be found (the vehicle cannot go in a straight line to any circle of radius $R_{\min}$ having a tangential point with the circle $\mathcal{C}(C_l,\ R_{\min})$). These poses are not representative of initial possible poses for a parking maneuver, e.g., when the vehicle is far from the parking spot (when $x_{E_{\text{init}}} \gg x_{C_l}$), with an almost vertical orientation. In those cases, a solution can be found by taking $R_{E_{\text{correct}}} \gg R_{\min}$ in (4), but as the parking maneuver would not be pertinent for those initial poses, the system would not allow it.

4) Feasibility of Parking in One Maneuver: The feasibility of parking in one maneuver is conditioned by the size of the parking spot: The length and the width have to be higher than the minimal length and width. This size is the same for retrieval or a parking maneuver. Supposing a retrieving maneuver, the maneuver is feasible if, during the first circle arc, the right front and rear corners of the vehicle have, respectively, no collision with the front and lateral obstacles (see Fig. 4). The necessary lateral free space is geometrically calculated by placing the vehicle at the left limit of the parking spot, and the minimal width $W_{\min}$ is deduced, i.e.,

$$W_{\min} = R_{A_l\min} - R_{\min} + b + d_l. \tag{6}$$

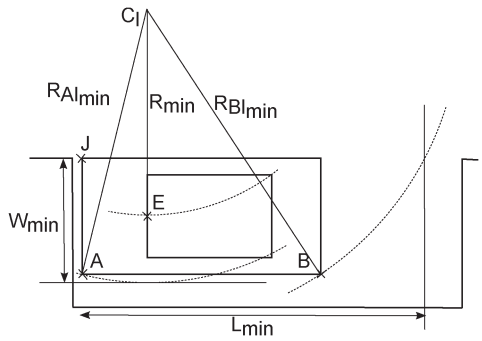

Fig. 4. Minimal length and width of the parking spot for parking in one maneuver.

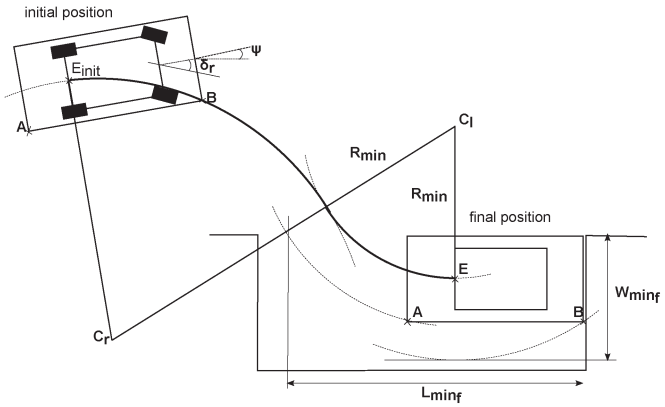

Fig. 5. Forward parking in one maneuver and minimal length and width of the parking spot.

In the case of parking near a sidewalk with clear space, the minimal width should even be calculated regarding the lateral deport of the right rear wheel instead of the right rear border of the vehicle. As the ICR is situated on the same axle than the rear track, we have in this case $W_{\min} = 2b + d_l + d_r = \text{Width}_{\text{car}}$. The minimum length $L_{\min}$ is deduced with a similar method, i.e., [19]

$$L_{\min} = d_{\text{rear}} + \sqrt{R^2_{B_l\,\min} - (R_{\min} - b - d_l)^2}. \quad (7)$$

5) Generalization to the Parallel Parking With a Forward Move: The presented method can be generalized to the parking done with a forward move. This forward parking can be used when the parking spot is known without scanning it by the vehicle, e.g., if an intelligent infrastructure has communicated this information previously to the vehicle. In that case, the vehicle is supposed to be parked before the parking spot, and retrieving is done first by left steering and then by right steering, connecting the real initial position of the vehicle, with a backward move (see Fig. 5). Then, this trajectory is reversed to park the vehicle with one forward maneuver. The minimal length and width of the parking are calculated with the same method as those used for backward parking (see Fig. 5), i.e.,

$$\begin{aligned} W_{\min_f} &= R_{B_l\,\min} - R_{\min} + b + d_l \\ L_{\min_f} &= a + d_{\text{front}} + \sqrt{R^2_{A_l\,\min} - (R_{\min} - b - d_l)^2}. \end{aligned} \quad (8)$$

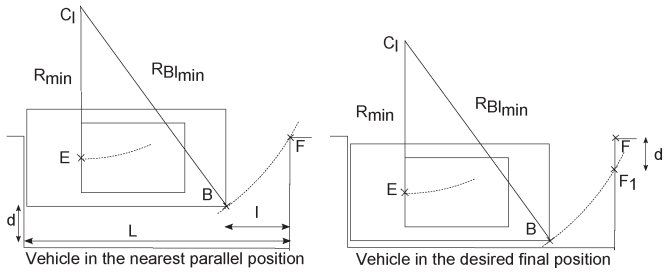

Fig. 6. Vehicle at the nearest parallel position to the parking spot after the first trial and vehicle in the desired final position.

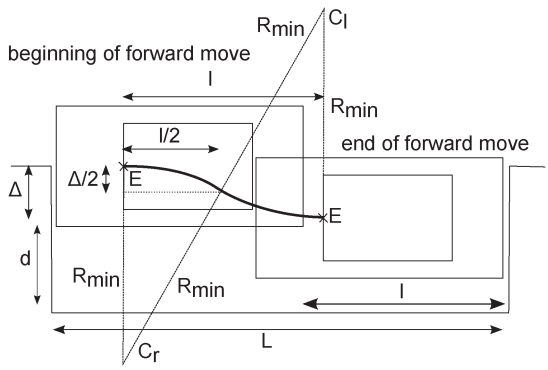

Fig. 7. Forward move during parking in n parallel trials.

B. Parking in Several Parallel Trials

When the length of the parking spot is smaller than the minimal length of the parking in one maneuver but the spot can contain the vehicle, parking in several trials can be performed. In this paper, we suppose that the vehicle performs backward parking in several trials (the first maneuver is a backward move), but this can be easily generalized for forward parking.

One solution for parking in several trials is first making the vehicle go to the nearest parallel position (see Fig. 6) to the parking spot using the one trial method. Then, the vehicle should execute a series of forward and backward moves to park in the spot (see Fig. 7). At the end of each of these moves, the vehicle has to be parallel to the spot.

1) Determine the Position at the End of the First Trial: During the first trial, the vehicle parks in the nearest parallel position to the parking spot (see Fig. 6). This means that, for the second circle arc of the parking maneuver, we have $d_{C_l B_{\text{parallel}}} = d_{C_l F} = R_{B_l\,\min}$. Having this circle arc, the first circle arc of the parking maneuver is calculated as in Section II. However, to know the second circle arc, the nearest parallel position has to be calculated, defined by the distance d between the vehicle at the nearest parallel position and the vehicle at the desired final position.

To calculate d, let us suppose that the vehicle is parked in the spot and tries to retrieve with a maximum steering angle. As the retrieval in one maneuver is not possible, the circle $\mathcal{C}(C_l,\, R_{Bl\,\min})$ and the front obstacle have a point of intersection F_1 (see Fig. 6). In these conditions, y_{F_1} can be easily calculated. Then, d is deduced: $d = y_F - y_{F_1}$.

2) Number of Trials: During the series of forward and backward moves, the vehicle covers longitudinally the available

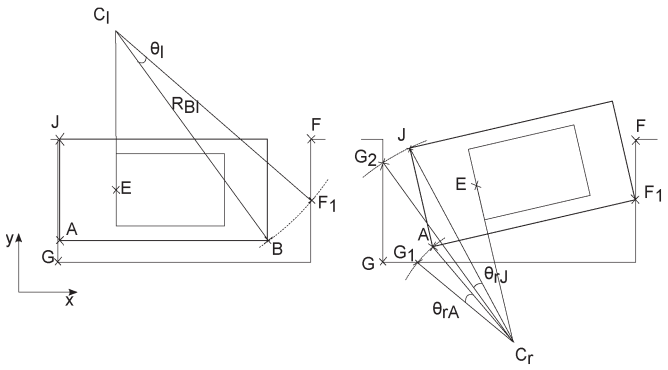

Fig. 8. Vehicle (left) moving forward and (right) backward with a maximum steering angle.

distance l, where $l = L - (a + d_{\text{front}} + d_{\text{rear}})$. During the first half distance, the steering is to the left, and during the second half distance, the steering is to the right (see Fig. 7). To remain parallel to the parking spot at the end of each move and to maximize lateral displacement, left and right steering angles must be maximal and equal. The lateral displacement during a forward or backward move is

$$\Delta = 2\left(R_{\min} - \sqrt{R_{\min}^2 - l^2/4}\right). \tag{9}$$

The total number of trials is deduced (first trial plus series of forward and backward moves) as

$$nb_{\text{trials}} = \text{IntegerPart}\left(\frac{d}{\Delta}\right) + 2. \tag{10}$$

Remark: For the last trial, the lateral distance to cover could be smaller than Δ. In this case, $R_{\min}$ is replaced by an appropriate radius in (9).

C. Parking in Several Reversed Trials

To find a parking spot in several trials, the method presented for the parking in one maneuver has been generalized. The retrieving path, like a human driver would do, is searched and then reversed. The retrieval is composed by forward and backward moves until the vehicle can retrieve. A forward move means steering at maximum toward left and then moving forward until approaching the front obstacle. A backward move means steering at maximum toward right and then moving backward until approaching the rear or lateral obstacle. When a forward move allows the vehicle to retrieve without collision, the concerned circle arc is considered. This will be the second circle arc of the parking path. Then, a feasible circle arc that connects by a tangential point the real initial position of the vehicle to the second circle arc is searched. The algorithm that finds the circle arcs of the retrieving maneuver is defined in the sequel.

1) It is assumed that the last pose of the vehicle when it is parked is known. This is the goal pose. C_l, C_r, $R_{B_l\min}$, and $R_{B_r\min}$ are calculated for this pose (see Fig. 8).
2) If $R_{B_l\min} \leq d_{C_lF}$, go to (8); else, go to (3).
3) It is not possible to retrieve in one trial. The vehicle moves forward with a maximum left steering angle. The created circle arc $\mathcal{C}(C_l,\, R_{B_l\min})$ crosses the line $x = x_F$ to a point F_1 (see Fig. 8). At the end of the movement, point B is in F_1. The rotation angle θ_l is deduced.
4) C_r is the ICR during the maximum right steering. Thus, it can be considered that it belongs to the vehicle. When the vehicle moves along the circle arc determined in the previous step, all points of the vehicle are transformed by the rotation of center C_l and angle θ_l.
5) The vehicle moves backward with a maximum right steering angle. The created circle arc $\mathcal{C}(C_r,\, R_{A_r\min})$ crosses the line $y = y_G$ to a point G_1 (see Fig. 8). Moreover, the created circle arc $\mathcal{C}(C_r,\, R_{J_r\min})$ crosses the line $x = x_G$ to a point G_2. The associated rotation angles θ_{rA} and θ_{rJ} are deduced. The vehicle must move backward as far as possible, but without collision. Consequently, it must stop when J is in G_2 or when A is in G_1. The corresponding circle arc is defined by $\theta_r = \min(\theta_{rA},\, \theta_{rJ})$.
6) C_l is the ICR during the maximum left steering. Thus, it can be considered that it belongs to the vehicle. When the vehicle moves along the circle arc determined in the previous step, all the points of the vehicle are transformed by the rotation of center C_r and angle θ_r.
7) A new d_{C_lF} is calculated, which brings us to step 2.
8) The vehicle can retrieve in one trial. The last two circle arcs of the retrieving maneuvers are found similar to the method for parking in one maneuver (see Fig. 9)

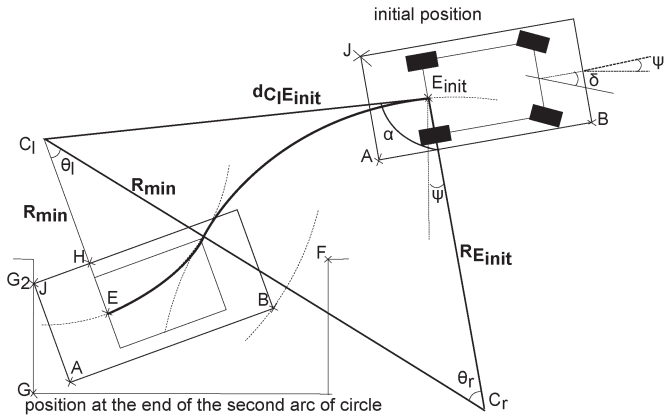

Fig. 9. Two arcs of the circle of the first trial during reversed parking in several trials.

IV. Continuous-Curvature Path for the Parking Maneuver

A. Choice of a Smooth Curve

Both geometric methods presented in the earlier section are particularly instinctive and adapted to the parking problem. However, as the path is composed of circle arcs, the curvature of the path is discontinuous. When the vehicle tracks such a path, it has to stop after each circle arc to reorient its front wheels. This can be undesirable for two reasons. First, as the vehicle has to stop, this leads to unnecessary time delay, as shown in [26], where a time comparison is performed between paths composed of circle arcs and paths using quintic polynomials. Second, steering at the stop is particularly demanding

to the steering column and induces faster wearing of the tires. The curvature continuity of the generated path is, therefore, a desirable property.

Different smooth curves can be used for creating a continuous-curvature path. Some curves are with coordinates that can be expressed in a closed form (e.g., B-splines [27], polar splines [28] or quintic polynomials). Others are parametric curves for which curvature is a function of their arc length (e.g., [29], clothoids [30], cubic spirals [31], or intrinsic splines [32]). An admissible path for a real vehicle has to include a constraint on the curvature (maximal steering angle) and on its derivative. The latter is upper bounded to reflect the fact that the vehicle can only reorient its front wheels with a finite velocity. It appears also that paths with continuous curvature and upper bounded curvature value and rate can be tracked with high accuracy by real vehicles [33].

However, the path-planning methods, which usually use continuous-curvature curves, often require optimization and a high computational cost (as presented in Section I). In comparison, the geometric methods present a lot of advantages (simplicity, no optimization needed, and no dependence on arbitrary chosen parameters). To reduce the complexity, an interesting method is to first create a geometrical path with circle arcs and then transform it in a continuous-curvature path with low computational cost. In [34], a method for parking in one maneuver using circle arcs and Bezier curve fitting is presented. Nevertheless, the admissibility of the created path is not guaranteed, and a complex controller is needed.

Clothoid paths can answer to the constraints of admissibility [35], [36]. Moreover, in [37], it was proved that the shortest path between two vehicle configurations with a constraint on the curvature rate is made up of line segments and clothoid arcs of maximum curvature derivative. Another argument in favor of the clothoids is that these curves describe very well the behavior of car-like vehicles. Indeed, if a car-like vehicle has a constant velocity and steers with a constant angular velocity, the middle of the rear track follows a clothoidal path. Consequently, simple control signals suffice for the vehicle to execute the path. For these reasons, in order to create continuous-curvature paths for car-like vehicles, the clothoids seems to be an appropriate solution. In the following, we propose to adapt geometric methods with circle arcs to methods that implement a clothoidal path.

B. Clothoid Turns

In this section, we briefly describe the general properties of clothoids applied to path planning for vehicles [36]. A clothoid is a curve whose curvature $\kappa = 1/R$ varies linearly with its arc length L, i.e., $\kappa(L) = \sigma L + \kappa(0)$, where σ is the sharpness of the clothoid. It is also commonly used to define a clothoid by its parameter A with $A^2 = RL$, where $A = 1/\sqrt{\sigma}$.

Without loss of generality, consider the start configuration of the vehicle as $q_i = (x_i, y_i, \psi_i, \delta_i) = (0, 0, 0, 0)$. The vehicle is moving with constant positive longitudinal velocity and with constant steering velocity to the left. The vehicle is then describing a clothoid whose parameter A depends on the longitudinal and steering velocities. The configuration for any pose

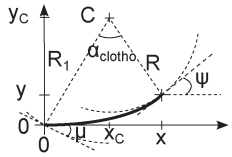

Fig. 10. Clothoid turns.

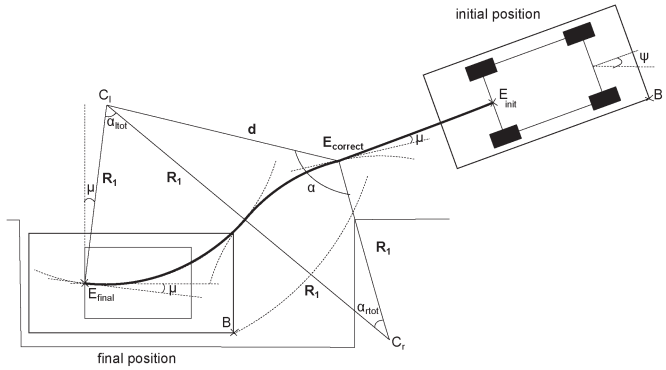

Fig. 11. Path for a parking in one maneuver.

q of the vehicle at distance L from the initial configuration is then (see Fig. 10) given as

$$q = \begin{cases} x = A\sqrt{\pi} C_f\left(\frac{L}{\pi A}\right) \\ y = A\sqrt{\pi} S_f\left(\frac{L}{\pi A}\right) \\ \psi = \frac{A^2}{2R^2} \\ \delta = \frac{1}{R} \end{cases} \tag{11}$$

where C_f and S_f are the Fresnel integrals $C_f(x) = \int_0^x \cos(\pi/2)u^2 du$ and $S_f(x) = \int_0^x \sin(\pi/2)u^2 du$, respectively.

The center of the circular arc C, located at a distance R from a configuration q, in the normal direction to the tangent to the clothoid at the $(x,\, y)$ point is

$$x_C = x_R - R\sin\psi \qquad y_C = y_R + R\cos\psi. \tag{12}$$

In addition, we define radius R_1 and angle μ between the orientation of q_i and the tangent to the circle of center C and radius R_1, i.e.,

$$R_1 = \sqrt{x_C^2 + y_C^2} \qquad \mu = \arctan\frac{x_C}{y_C}. \tag{13}$$

Then, we define a clothoidal sequence $CAC(A, L, \theta)$ as follows:

1) clothoid of parameter A, of length L, of initial null curvature, and of end curvature equal to $1/R$;
2) optional arc of circle of radius R and of angle θ;
3) clothoid of parameter A, of length L, of initial curvature equal to $1/R$, and of end null curvature.

In the method presented in the following, R_1 represents the distance from the point E at the beginning of a circle arc of the geometric path to the ICR C (see Fig. 11). To make the most of the maximal steering angles of the vehicle, we want radius R_1 to be as small as possible. The minimal time to steer from null steering to maximal steering is $t_{\min} = (\delta_{\max}/v_\delta)$, where v_δ is the maximal desired steering velocity. The minimal associated

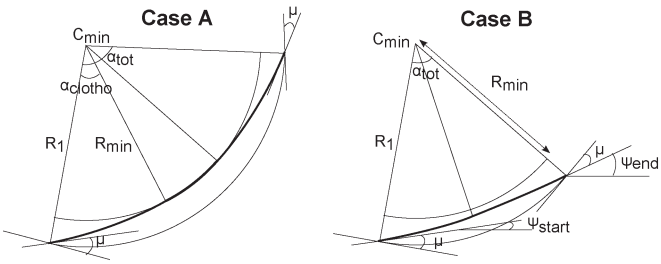

Fig. 12. Replacing of a circle arc by an A or B sequence.

length of the path is then defined as $L_{\min} = v_{\text{longi}} t_{\min}$, where v_{longi} is the maximal desired longitudinal velocity. The parameter of the used clothoid is then given as $A^2_{\min} = R_{\min} L_{\min}$, and R_1 is calculated using (11)–(13). Let α_{clotho} be the angle formed by a clothoid started with a null curvature and finished with a curvature $1/R_{\min}$.

C. Approach of Computing the Continuous-Curvature Path

The first step of the parking path generation is to create a geometric path composed of circle arcs, e.g., with one of the methods presented in the earlier section, for parking in single or more maneuvers. Radius $R_{\min}$ used to create this path is replaced here by radius R_1. Another modification concerns the ICR C. In the geometrical methods, this is located on the same line with that of the rear track. This means that the orientation of the vehicle is tangent in E to the circle arc of the geometric path. In this new strategy, in order to use clothoids, the orientation of the vehicle always presents angle μ with the tangent to the circle in E, when the vehicle is situated on the circles of radius R_1 of the geometric path. To take this constraint into account, C is transformed by the rotation of center E and angle μ during the geometric path generation (see Fig. 11).

Remark: In the new approach, with circle arcs of radius R_1, in the case of parking near a sidewalk with clear space, the lateral deport of the vehicle's right rear for the retrieving in one maneuver is no longer null. This is due to the fact that the center C of the circle arc of radius R_1 is no longer situated on the same axle as the rear track. In consequence, the minimal width of the spot is no longer equal to the width of the vehicle, but slightly larger.

The second step is to transform each circle arc of angle α_{tot} and radius R_1 of the geometric method into a clothoidal sequence. Three cases are classically considered [35] (see Fig. 12 for the cases A and B).

Case A) $\alpha_{\text{tot}} \geq 2\alpha_{\text{clotho}}$*:* We use the clothoidal sequence $CAC(A_{\min}, L_{\min}, \alpha_{\text{tot}} - 2\alpha_{\text{clotho}})$.

Case B) $2\alpha_{\text{clotho}} > \alpha_{\text{tot}} \geq 2\mu$*:* We use the clothoidal sequence $CAC(A_{\text{new}}, L_{\text{new}}, 0)$ with [35]

$$A_{\text{new}} = \sqrt{\frac{R_1^2 \sin\left(\frac{\beta}{2} + \mu\right)^2}{\pi \left(\cos\frac{\beta}{2} C_f\left(\sqrt{\frac{\beta}{\pi}}\right) + \sin\frac{\beta}{2} S_f\left(\sqrt{\frac{\beta}{\pi}}\right)\right)^2}} \tag{14}$$

$$L_{\text{new}} = A_{\text{new}} \sqrt{\beta} \tag{15}$$

where $\beta = (\psi_{\text{end}} - \psi_{\text{start}}) \bmod 2\pi$ is the deflection of the turn.

Case C) $\alpha_{\text{tot}} < 2\mu$*:* In this case, it is no longer possible to use the method of the case B, and although this case is not dealt with in [35], left steering is still possible. A clothoid of parameter $A_{\min}$ and of length L_{caseC} is calculated to satisfy the following two criteria: $\alpha_{\text{tot}} = 2\alpha_{\text{clothocaseC}}$, and at the end position, it is no longer possible to go forward (or backward, depending on the case) without a collision. As this calculus includes parametric curves with Fresnel integrals, an approached solution is considered. Finally, the sequence $CAC(A_{\min}, L_{\text{caseC}}, 0)$ is used.

The last step is to calculate the starting point of the first circle arc. As aforementioned, to minimize the lateral offset, only circles of radius R_1 are considered during the first step of the strategy. In consequence, the vehicle has to go backward or forward without steering from its initial position E_{init} until it arrives at a point E_{correct} on a circle of radius R_1 connected with a tangential point to the second circle (see Fig. 11). The coordinates of E_{correct} can be calculated by applying the Al-Kashi theorem to the triangle $C_l C_r E_{\text{correct}}$[21], i.e.,

$$3R_1^2 - d^2 + 2dR_1 \cos\alpha = 0 \tag{16}$$

with

$$\begin{cases} d = \sqrt{(x_{Cl} - x_{E_{\text{correct}}})^2 + (y_{Cl} - y_{E_{\text{correct}}})^2} \\ \alpha = \arccos\frac{y_{E_{\text{correct}}} - y_{Cl}}{d} - \mu + \psi_{E_{\text{init}}} \\ y_{E_{\text{correct}}} = y_{E_{\text{init}}} - (x_{E_{\text{init}}} - x_{E_{\text{correct}}}) \tan\psi_{E_{\text{init}}}. \end{cases} \tag{17}$$

D. Feasibility of Parking in One Maneuver

Similar to the first presented geometric method, the feasibility of parking in one maneuver is conditioned by the size of the parking spot. The conditions issued from the initial geometric path planning with circle arcs of radius R_1 are conditions of noncollision of extremities of the vehicle with the spot borders, when the point E follows the circle arcs of radius R_1. With the continuous-curvature solution presented in this section, those conditions have to be modified. During the parking maneuver, the vehicle travels between two extremal circles of center C_l and of radius $R_{\min}$ or R_1. This creates a lower bound and an upper bound of the minimal length $L_{\text{minclotho}}$ and the minimal width $W_{\text{minclotho}}$ of the parking spot, with which the parking in one trial is possible (18). The minimal width, as it is very close to the width of the vehicle, is rarely an issue for parallel parking. The real difficulty, with a growing number of maneuvers, comes from the length of the spot, as L_{limmin} and L_{limmax} increase when R_1 increases. Consequently, when possible, the interesting parameter to optimize is the minimal length of the spot for the parking in one maneuver (and by generalization, the minimal length of the spot for a parking in a given number of maneuvers). By construction, R_1 decreases when the maximal desired longitudinal velocity v_{longi} decreases and when the maximal desired steering velocity v_δ increases, i.e.,

$$\begin{aligned} L_{\text{limmin}} &\leq L_{\text{minclotho}} \leq L_{\text{limmax}} \\ W_{\text{limmin}} &\leq W_{\text{minclotho}} \leq W_{\text{limmax}} \end{aligned} \tag{18}$$

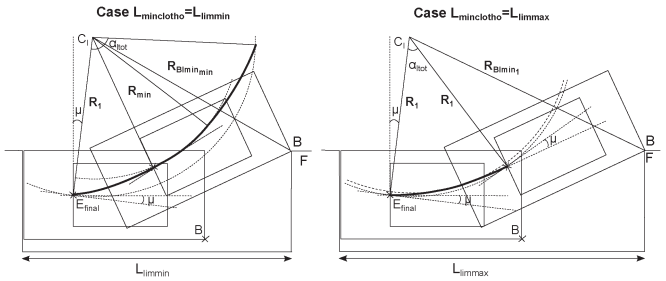

Fig. 13. Cases with (left) lower and (right) upper bounds for the minimal length of the parking spot for the parking in one maneuver.

where

$$\begin{aligned} L_{\text{limmin}} &= d_{\text{rear}} + R_1 \sin\mu \\ &\quad + \sqrt{R^2_{B_l \min_{\min}} - (R_1\cos\mu - b - d_l)^2} \\ L_{\text{limmax}} &= d_{\text{rear}} + R_1 \sin\mu \\ &\quad + \sqrt{R^2_{B_l \min_1} - (R_1\cos\mu - b - d_l)^2} \\ W_{\text{limmin}} &= R_{A_l \min} - R_1\cos\mu + b + d_l \\ W_{\text{limmax}} &= R_{A_l \min_1} - R_1\cos\mu + b + d_l \end{aligned} \tag{19}$$

with

$$\begin{aligned} R_{B_l \min_{\min}} &= \sqrt{R^2_{\min} + d^2_{EB} - 2R_{\min} d_{EB}\cos(\pi/2 + \alpha_B)} \\ R_{B_l \min_1} &= \sqrt{R^2_1 + d^2_{EB} - 2R_1 d_{EB}\cos(\pi/2 + \alpha_B + \mu)} \\ R_{A_l \min_1} &= \sqrt{R^2_1 + d^2_{EA} - 2R_1 d_{EA}\cos(\pi/2 + \alpha_A + \mu)} \\ \alpha_B &= \arccos\frac{a + d_{\text{front}}}{d_{EB}} \\ \alpha_A &= \arccos\frac{d_{\text{rear}}}{d_{EA}}. \end{aligned} \tag{20}$$

Cases with $L_{\text{minclotho}} = L_{\text{limmin}}$ and with $L_{\text{mincloto}} = L_{\text{limmax}}$ are presented in Fig. 13.

Remark: If $R_1 = R_{\min}$ (clothoid formed when $v_{\text{longi}} = 0$ or $v_\delta = \infty$), the minimal length and width become those of the minimal ones in the geometric method.

V. Discussion

A. Parameters of the Vehicle

The parameters chosen for the simulation of the different generation methods of the trajectory are the Renault ZOE parameters (see Table I). The maximal steering velocity of the steering wheels chosen for the parking maneuvers is $v_{\text{delta}} = 20^\circ/\text{s}$.

B. Minimal Length and Width of the Parking Spot for Parking in One Maneuver (Forward or Backward)

It is interesting to compare the minimal width and length of the spot for forward and backward parking in one maneuver

TABLE I
Model of the Used Vehicle

Parameters	*Notation*	*Value*
Wheelbase	a	2588 mm
Track	2b	1511 mm
Front overhang	d_{front}	839 mm
Rear overhang	d_{rear}	657 mm
Distance from the left, right wheel to the left, right side of the vehicle (exterior mirrors folded)	d_l,d_r	130 mm
Maximum left, right steering angle	δ_{lmax},δ_{rmax}	33 ^{o}
Total length of the vehicle	$l_{vehicle}$	4084 mm
Total width of the vehicle	$w_{vehicle}$	1771 mm

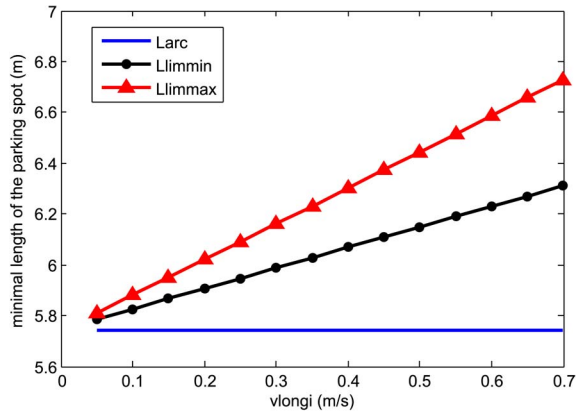

Fig. 14. Variation of minimal length of the parking spot for $v_\delta = 20^\circ/\text{s}$.

with a geometric path formed by circle arcs [see (6)–(8)]. With the parameters of the Renault ZOE, $W_{\min} = 1.815$ m, $L_{\min} = 5.742$ m, $W_{\min_f} = 2.856$ m, and $L_{\min_f} = 7.241$ m. Forward parking needs a consequent width of the spot in comparison with backward parking, for which the minimal width of the spot is very close to the width of the vehicle (see Table I). In the case of parking near a sidewalk with clear space, the minimal width of the spot for forward parking stays consequent. With backward parking, it is equal or almost equal to the width of the vehicle. Furthermore, the minimal length is also consequently higher for forward parking. Nevertheless, forward parking can be an interesting option for time saving when the dimensions of the parking spot are suitable: With this method, the parking maneuver can begin immediately without having to travel near the spot to scan it and thereafter only begin the parking maneuver, like in backward parking. Until the end of this paper, the calculations and experiments will be done only for backward parking.

It is also interesting to compare the minimal length of the spot for parking in one maneuver on one hand with a geometric path formed by circle arcs $L_{\min}$ (7) and on the other hand with a continuous-curvature path with CAC sequences. The latter minimal length $L_{\text{minclotho}}$ is characterized by its bounds L_{limmin} and L_{limmax} in (19). Fig. 14 shows the variation of L_{limmin} and L_{limmax} in function of the longitudinal velocity for $v_\delta = 20^\circ/\text{s}$. These lengths are larger than L_{arc}, but they considerably decrease when v_{longi} decreases. Nevertheless, these minimal lengths are acceptable considering that the parking in several maneuvers is possible and that continuous-curvature path is preferable.

TABLE II
NUMBER OF MANEUVERS FOR DIFFERENT GEOMETRIC METHODS FOR PARKING IN A SPOT WITH A WIDTH OF 2 m AND OF DIFFERENT LENGTHS

Length (m)	5.75	5.60	5.44	5.34	4.92	4.79	4.75
Parallel method	1	3	5	7	26	39	45
Reversed method	1	3	3	3	3	5	7

TABLE III
NUMBER OF MANEUVERS IN FUNCTION OF THE LENGTH OF THE SPOT FOR DIFFERENT WIDTHS FOR CONTINUOUS-CURVATURE PATH PLANNING

Nb trials	1	3	5	7	9
Length (m) for width 2,00m	6.24	5.80	5.75	5.742	5.741
Length (m) for width 2,50m	6.24	5.64	5.51	5.46	5.43

C. Comparison of the Path-Planning Methods for Several Trials

We have presented two geometric methods with circle arcs for parallel parking in one or several trials: the parallel and the reversed methods. In this section, we compare these methods regarding the number of maneuvers needed to park the vehicle in tiny spots. We take as reference, e.g., the French standard for parallel parking spots, which should be in minimum 2 m $\times$ 5.8 m [38].

The method with several parallel trials is simple to implement, and the number of trials is easily calculated from the geometry of the vehicle and the parking spot. Moreover, if a passenger is present in the vehicle, it is easy for him to understand and predict the maneuvers of the vehicle. Furthermore, the number of maneuvers does not depend on the width of the parking spot. Nevertheless, if the width of the parking spot is too small, the lateral deport of the front and rear right corners of the vehicle makes parking near a wall impossible for some parking length. For example, it would be impossible to use this method for a parking spot with a width of 2 m and a length of 5.64 m. Let us suppose that the spot is not situated near a wall or near an obstacle. In that case, parking in a spot with a width of 2 m is possible; the number of maneuvers is presented in Table II. We can see that the condition of displacement with the beginning and end of each move, being parallel to the parking spot, is very restraining: The total number of trials increases very fast when the length of the parking decreases, which can be unsatisfactory if a passenger is present in the vehicle or for the total needed time.

The method with several reversed trials is instinctive to implement because it correlates with reversing the human retrieving maneuver. With this method, the number of trials can be calculated only from an iterative algorithm. Geometric transformations and formulas involved in the algorithm are more complex in comparison with the method in several parallel trials, and the number of maneuvers depends on the width of the parking spot. Moreover, for a human, it is not easy to visualize which trajectory the vehicle will generate. Nevertheless, the number of trials implied in this method is much less considerable than in the method with several parallel trials (see Table II). Consequently, this method is to be used in priority in order to reduce the time of the parking maneuver.

As the reversed method is the most efficient, it is interesting to use it for the continuous-curvature path planning. With this transformation, the length of the parking spot should increase in order to park with the same number of maneuvers than with a path done with circle arcs. As the reversed method depends on the width of the parking spot, here, the phenomenon is accentuated if the parking has to be done near a wall. An example of the minimal lengths of the parking spot for a longitudinal speed of 0.6 m $\cdot$ s^{-1} for parking near a wall for different widths of the spot is shown in Table III. Even if these lengths are larger than that for geometric parking with circle arcs, it is always possible to park in an acceptable number of maneuvers in spots with length smaller than 5.8 m, even for parking near a wall. If the parking spot is very tiny, as it can occur in big cities, the steering at stop can always be considered with the reversed geometric method with circle arcs. In that case, it is even possible to park in a spot that is only 80 cm larger than the length of the vehicle in a reasonable number of maneuvers (see Tables I and II).

VI. CONTROL SIGNALS AND POSE ESTIMATION

A. Control Signals

To make the vehicle follow the generated path, control signals of the steering angle δ and longitudinal velocity v have to be built. As the trajectory is clothoidal, the calculation of trajectory coordinates implies an approximation of Fresnel integrals, which requires much calculation time. Instead, we propose to generate open-loop steering and braking controls (Step 3 of Fig. 1), which depend only on the traveled distance and need few calculations, as shown in the following.

The speed control purpose is that the vehicle accelerates to a desired speed and then stays at this speed to finally decelerate and stop when the vehicle has traveled the total distance of a forward move or a backward move. This control signal could be a trapezoid signal.

For the steering control signal, the vehicle has already stored some information during the path-planning routine: L_{line}, the length of the first line with straight wheels, $R_{\min}$ and the parameters A, L, θ for each clothoidal sequence $CAC(A, L, \theta)$. Therefore, the length of a circle arc on a clothoidal sequence is $L_{\text{arc}} = \theta R_{\min}$, and the total length of a clothoidal sequence is $L_{\text{seq}} = 2L + L_{\text{arc}}$. Whatever the number of clothoidal sequences A or C (see Section III) is, the parameter A has to be calculated only once. Moreover, the parameter A has to be calculated every time a sequence B occurs. Consequently, the amount of data calculated and stored for the steering control is directly related to the number of maneuvers. Finally, the distance control signal of the steering angle is as follows.

– For the initial movement in a straight line

$$\forall d \in (0, L_{\text{line}}) \quad \delta(d) = 0. \tag{21}$$

– For a clothoidal sequence $CAC(A, L, \theta)$: $\forall d \in (0, L_{\text{seq}})$

$$\delta(d) = \begin{cases} k_\delta \left|\arctan \frac{a}{R}\right| & d \in [0, L] \\ k_\delta \left|\arctan \frac{a}{R_{\min}}\right| & d \in]L, L + L_{\text{arc}}[\\ k_\delta \left|\arctan \frac{a}{R_i}\right| & d \in [L + L_{\text{arc}}, L_{\text{seq}}] \end{cases} \tag{22}$$

where $k_\delta = \pm 1$ corresponds to left $(+1)$ or right (-1) steering, $R = (A^2/d)$ and $R_i = (A^2/L_{\text{seq}} - d)$.

B. Pose and Distance Estimation

The different internal sensors present on the vehicle allow to measure the steering wheel angle δ and the four wheel speeds (ABS sensors present in modern cars). The elementary lateral displacements $\Delta_{RR}, \Delta_{RL}, \Delta_{FR}, \Delta_{FL}$ of rear right, rear left, front right, and front left wheels, respectively, are deduced. Exteroceptive sensors for environment perception are beyond the scope of this paper. Consequently, we propose odometric techniques for the estimation of the pose and the traveled distance.

The most common technique uses only the speed of the two rear wheels. The elementary angular displacement ω and the elementary lateral displacement Δ are classically calculated at each time step k

$$\Delta = \frac{\Delta_{RR} + \Delta_{RL}}{2} \qquad \omega = \frac{\Delta_{RR} - \Delta_{RL}}{2b}. \tag{23}$$

It is also possible to make a fusion of all available measurements using an odometric extended Kalman filter (EKF) [39] where the unknown quantities $x = (\Delta, \omega)$ are linked to the measured variables $y = (\Delta_{FL}, \Delta_{FR}, \Delta_{RL}, \Delta_{RR}, \delta)$ by a redundant and nonlinear system

$$\begin{cases} \tan(\delta) = \frac{a\omega}{\Delta} \\ \Delta_{RL} = \Delta - b\omega \\ \Delta_{RR} = \Delta + b\omega \\ \Delta_{FL}\cos(\delta_l) = \Delta - b\omega \\ \Delta_{FR}\cos(\delta_r) = \Delta + b\omega \end{cases} \tag{24}$$

where $\delta_l = \arctan(\tan(\delta)a/(a - \tan(\delta)b))$ and $\delta_r = \arctan(\tan(\delta)a/(a + \tan(\delta)b))$ are the steerings of the front left and right wheels (see Fig. 2). Thus, we can write the Kalman filter

$$x_{k+1} = x_k + w_k \tag{25}$$

where w is a zero-mean white noise with a W covariance matrix.

The distance estimation d and the pose of the vehicle (x, y, ψ) are then deduced for the next time step as

$$\begin{aligned} d_{k+1} &= d_k + \hat{\Delta}_k \\ x_{k+1} &= x_k + \hat{\Delta}_k \cos(\psi_k + \hat{\omega}_k/2) \\ y_{k+1} &= y_k + \hat{\Delta}_k \sin(\psi_k + \hat{\omega}_k/2) \\ \psi_{k+1} &= \psi_k + \hat{\omega}_k \end{aligned} \tag{26}$$

with $(\hat{\Delta}, \hat{\omega})$ being the estimates of the Kalman filter.

VII. Experimental Results

A. Vehicle and Ground Truth Sensors

The car used for experiments is a Renault ZOE with automatic speed and steering control (see Fig. 18). The sources of errors that affect the pose estimation and the result of the parking maneuver are numerous. The first one is due to the resolution of the ABS encoders and the steering wheel encoder. The other ones result from the approximate nature of the Ackerman model (cinematic model without sliding) and from the performance of the speed and steering response to the control signals (the car was not particularly prepared for low speed maneuvers).

First, simulations on MATLAB were performed for different scenarios. Moreover, all algorithms were integrated in a complete MATLAB Simulink model allowing automatic control of the car. The implementation of this model in the vehicle was operated due to dSPACE MicroAutoBox, a real-time system for performing fast prototyping. Then, some of the simulated scenarios with a maximal longitudinal speed 0.6 $\mathrm{m \cdot s^{-1}}$ were tested (Fig. 19 compares some simulated scenarios to the real experiments, as explained in the Section VII-C).

Two sensors allow the measurement of the ground truth. A GPS RTK delivers true positions of the car with a precision of 2 cm, and a Correvit is used to measure the odometry of the rear track center with a resolution of 1.9 mm and a measurement deviation less than $\pm 0.1\%$.

B. Pose and Distance Estimation

The experimental results presented here were obtained during automatized parking maneuvers using continuous-curvature path planning outgoing from the reversed geometric method. The control signals presented in the previous section have been implemented. The distance measurement for the control signals was produced by the Correvit but simultaneously, the distance measurement and the pose estimation were also calculated online. The techniques tested for pose estimation are using the two rear wheel sensors (classic odometry) and the odometric EKF with the fusion of all wheels and steering measurements. In both techniques, the calculated elementary longitudinal displacement is used for the distance estimation.

The pose and distance estimation were tested on different ground conditions (asphalt and concrete slab as good ground conditions, and gravel and wet concrete slab as difficult ground conditions) for parking in one or several maneuvers. Results are shown in Figs. 15 and 16 with a top view representation. In these figures also visible are the distance error (with respect to the Correvit) and the longitudinal and lateral errors (with respect to the GPS RTK) as functions of the real traveled distance (given by the Correvit). The distance estimation with the classic odometry method is correct for all ground conditions (generally less than 10 cm of difference). For the distance calculated with the EKF method, the results are more controversial: They are correct on good ground conditions, but fail on wet ground and gravel (errors of 20–50 cm at the end of the maneuver). Similarly, the pose estimation is always correct for the classic odometry and becomes degraded for the EKF method on difficult ground conditions.

It should be noticed that, by changing the covariance matrices of the EKF, we can obtain the same performances than with the classic odometry, but not a better one. This could be due to the slipping of the front wheels during low-speed movements with consequent steering angles. Another explanation is that, during our experiment, the information provided by the sensors of the rear wheels was not corrupted; hence, the classic odometry performed very well. In [39], the EKF was tested

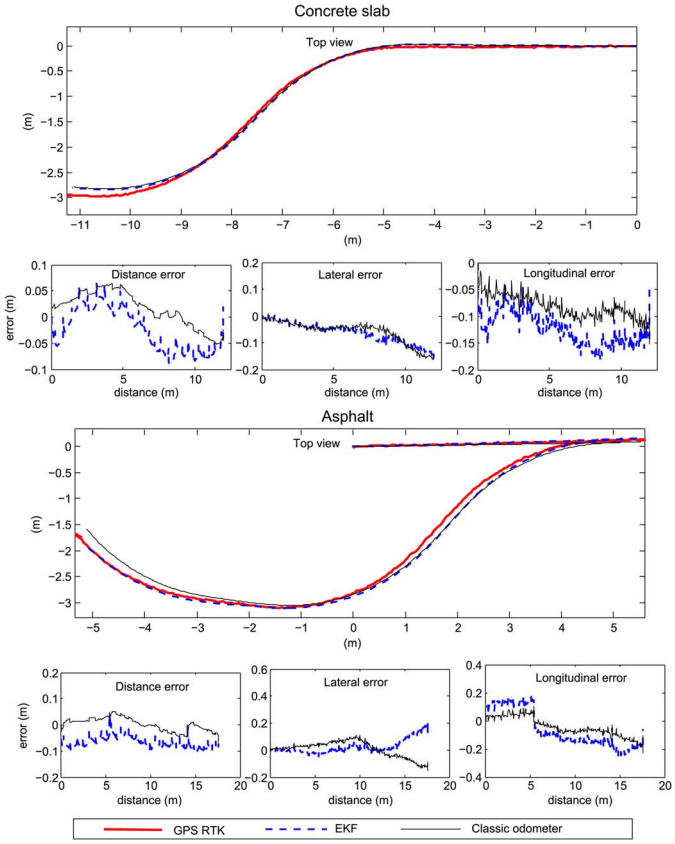

Fig. 15. Pose and distance estimation for the experiments on good ground conditions.

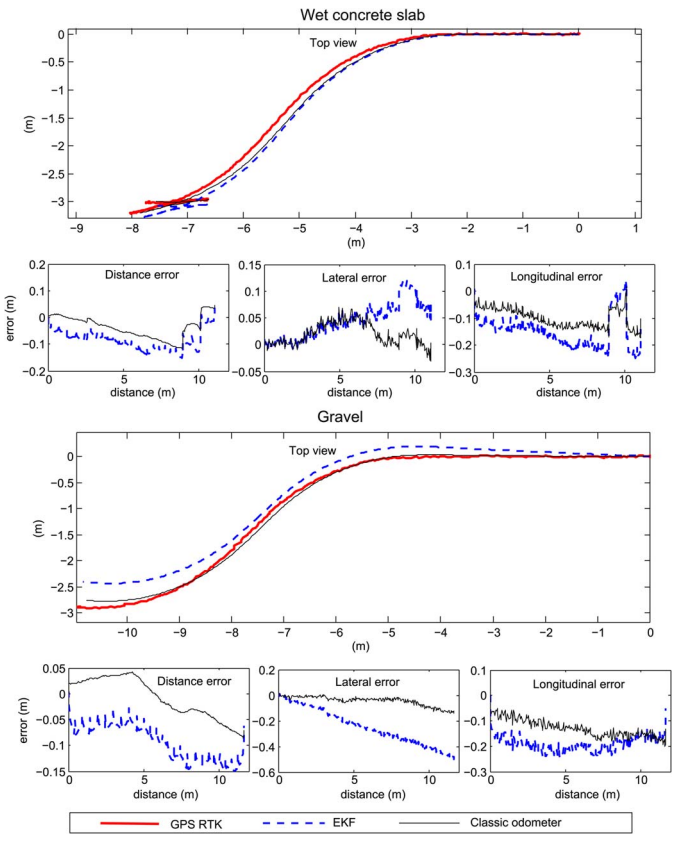

Fig. 16. Pose and distance estimation for the experiments on difficult ground conditions.

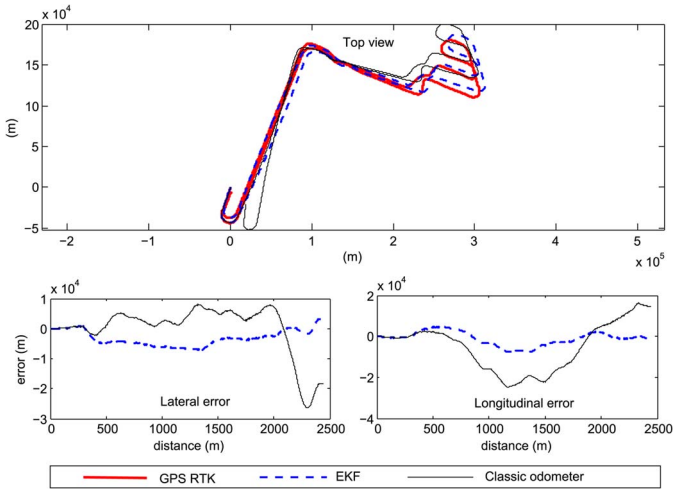

Fig. 17. Pose estimation for a long travel on the road.

with a maximum speed of 50 km/h without maximum steering angles during long travels on the road, and in that situation, the classic odometer alone was less efficient than the EKF estimation. To verify our EKF, we tested it in similar conditions with [39] and observed that it performs much better than the classic odometry during these kind of runs (see Fig. 17). In the case of parking maneuvers, the classic odometer provides good results without large failures and consequently the benefits of the EKF (reduction of the error during failures or noises of one or several sensors) cannot be seen. If exteroceptive information is available on the vehicle or if a more complex vehicle model, including wheels slip and adaptation to low-speed movement and big steering angles, would be used, the EKF could be more efficient. Nevertheless, classic odometry shows good results on all experiments for pose and distance estimation without any other information and consequently validate an approach with the use of few sensors.

C. Parking Maneuvers

Regarding the results of pose and distance estimation, the automatic parking was tested with distance control issued from the classic odometry. We have tested the parking in one or several maneuvers and with different initial positions and orientations. The width of the parking spot was 2.50 m, and the parking maneuvers were tested without lateral overtaking of the right corners of the vehicle (parking near a wall).

Fig. 18 shows the different steps of parking in four maneuvers. Picture (a) represents the initial position of the vehicle, picture (b) shows the end of the first maneuver, picture (c) is taken during the entrance in the parking spot, picture (d) represents the end of the second maneuver, picture (e) shows the end of the third maneuver and finally, the end of the parking is on picture (f). Fig. 19 shows the real trajectories of the vehicle during automatic parking compared with the simulated ones.

The experimental results are quite good, and the errors are mainly due to the execution delay of the control signals and the errors of distance estimation. Despite the differences between the simulations and the ground truth, for the parking in two to four maneuvers, the vehicle never exceeded the parking spot,

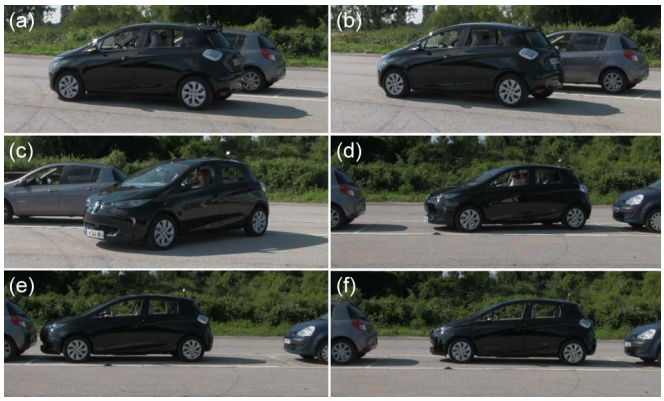

Fig. 18. Parking in four maneuvers.

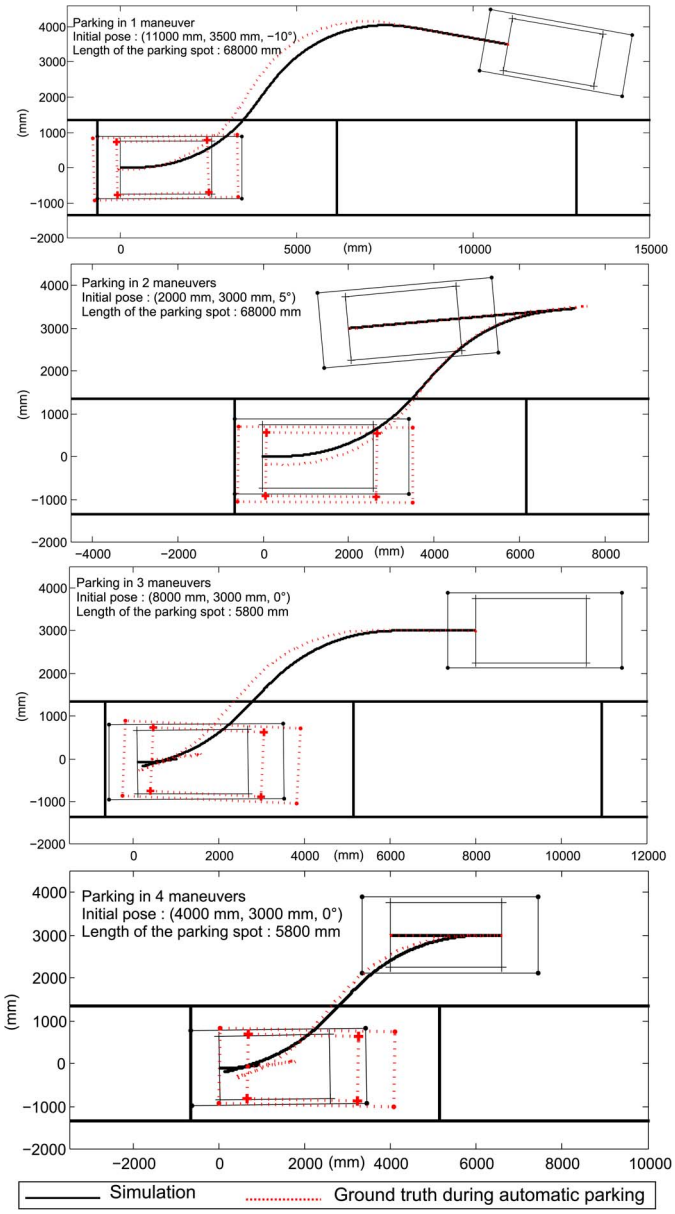

Fig. 19. Experiments of parking maneuvers.

and the end position is suitable. For the parking in one maneuver, the errors (mainly delay error) cause a little overstep, but that can be corrected using low-cost sensor, such as ultrasounds. For parking in more than four maneuvers (not shown here), the accumulation of errors becomes too big to correctly park the vehicle. Future work on the regeneration of the trajectory should solve this problem.

VIII. Conclusion

A complete approach of a full automatic parallel parking was proposed. The functional dependence of the perception, path planning, and trajectory tracking, including emergency stop routine and conditions at the end of the maneuver have been highlighted. Then, the path-planning method was detailed. First, two geometrical methods and an extension to the forward parking have been presented. Second, an extension of those trajectories to continuous-curvature trajectories has been added. These path-planning methods allow the parking in one or several maneuvers in tiny spots for any initial pose and orientation. Control signals for steering, braking, and acceleration allowing to control the vehicle without calculation of points on the trajectory were then detailed. Moreover, it has been shown that classic pose and distance estimation allows a correct localization and produces precise distance information for the control signals. Experiments of the parking in one or several maneuvers on a real vehicle confirm the chosen approach of the path planning and of the vehicle control. In the future, online regeneration of the trajectory will be performed in order to prevent error accumulation. This regeneration will have the same function as a closed-loop control in order to have better precision during the execution of the maneuver. To reduce the error sources that affect the pose estimation, the low-level control signals of the car have to be improved to take into account the low-speed movement, and a model including the sliding of the wheels will be considered.

Acknowledgment

The authors would like to thank F. Desnoyer for his support to organize the experiments and B. Lusetti for his precious help during the experiments.

References

[1] S. Lee, M. Kim, Y. Youm, and W. Chung, "Control of a car-like mobile robot for parking problem," in *Proc. IEEE Int. Conf. Robot. Autom.*, Detroit, Michigan, USA, May 1999, pp. 1–6.

[2] I. E. Paromtchik, P. Garnier, and C. Laugier, "Autonomous maneuvers of a nonholonomic vehcicle," in *Proc. Int. Symp. Exp. Robot.*, Barcelona, Spain, Jun. 1997, pp. 277–288.

[3] Y. Zhao and E. G. Collins, "Robust automatic parallel parking in tight spaces via fuzzy logic," *Robot. Auton. Syst.*, vol. 51, no. 2–3, pp. 111–127, May 2005.

[4] R. E. Jenkins and H. P. Yuhas, "A simplified neural network solution through problem decomposition: The case of the truck backer-upper," *IEEE Trans Neural Netw.*, vol. 4, no. 4, pp. 718–720, Jul. 1993.

[5] F. Gomez-Bravo, F. Cuesta, and A. Ollero, "Parallel and diagonal parking in nonholonomic autonomous vehicles," *Eng. Appl. Artif. Intell.*, vol. 14, no. 4, pp. 419–434, Aug. 2001.

[6] C.-K. Lee, C.-L. Lin, and B.-M. Shiu, "Autonomous vehicle parking using artificial intelligent approach," in *Proc. Int. Conf. Auton. Robots Agents*, Wellington, New Zealand, Feb. 2009, pp. 496–501.

[7] T. Ozkul, M. Mukbil, and S. Al-Dafri, "A fuzzy logic based hierarchical driver aid for parallel parking," in *Proc. Int. Conf. Artif. Intell., Knowl. Eng. Data Bases*, U.K., Feb. 2008, pp. 357–361, University of Cambridge.

[8] Y.-W. Ryu, S.-Y. Oh, and S.-Y. Kim, "Robust automatic parking without odometry using an evolutionary fuzzy logic controller," *Int. J. Control, Autom., Syst.*, vol. 6, no. 3, pp. 434–443, Jun. 2008.

[9] K. Kondak and G. Hommel, "Computation of time optimal movements for autonomous parking of non-holonomic mobile platforms," in *Proc. IEEE Int. Conf. Robot. Autom.*, Seoul, Korea, May 2001, pp. 2698–2703.

[10] M. B. Oetiker, G. P. Baker, and L. Guzzella, "A navigation-field-based semi-autonomous nonholonomic vehicle-parking assistant," *IEEE Trans. Veh. Technol.*, vol. 58, no. 3, pp. 1106–1118, Mar. 2009.

[11] P. Jacobs, J. P. Laumond, and M. Taix, "Efficient motion planners for nonholonomic mobile robots," in *Proc. IEEE/RJS Int. Work. Intell. Robots Syst.*, Osaka, Japan, Nov. 1991, pp. 1229–1235.

[12] J. P. Laumond, P. E. Jacobs, M. Taix, and R. M. Murray, "A motion planner for nonholonomic mobile robots," *IEEE Trans. Robot Autom.*, vol. 10, no. 5, pp. 577–593, Oct. 1994.

[13] B. Mueller, J. Deutscher, and S. Grodde, "Continuous curvature trajectory design and feedforward control for parking a car," *IEEE Trans. Control Syst. Technol.*, vol. 15, no. 3, pp. 541–553, May 2007.

[14] K. Chend, Y. Zhang, and H. Chen, "Planning and control for a fully-automatic parallel parking assist system in narrow parking spaces," in *Proc. IEEE Int. Symp. Intell. Veh.*, Gold Coast, Australia, Jun. 2013, pp. 1440–1445.

[15] A. Gupta and R. Divekar, "Autonomous parallel parking methodology for Ackerman configured vehicles," in *Proc. of Int. Conf. Control, Commun. Power Eng.*, Chennai, India, Jul. 2010, pp. 22–27.

[16] T. Inoue, M. Q. Dao, and K.-Z. Liu, "Development of an auto-parking system with physical limitation," in *Proc. SICE Annu. Conf.*, Sapporo, Japan, Aug. 2004, pp. 1015–1020.

[17] K. Jiang, D. Z. Zhang, and L. D. Seneviratne, "A parallel parking system for a car-like robot with sensor guidance," *Proc. Inst. Mech. Eng. Part C: J. Mech. Eng. Sci.*, vol. 213, no. 6, pp. 591–600, Jun. 1999.

[18] Y. K. Lo, A. B. Rad, C. W. Wong, and M. L. Ho, "Automatic parallel parking," in *Proc. IEEE Conf. Intell. Transp. Syst.*, Shanghai, China, Oct. 2003, pp. 1190–1193.

[19] S. Choi, C. Boussard, and B. d'Andrea Novel, "Easy path planning and robust control for automatic parallel parking," in *Proc. 18th IFAC World Congr.*, Milano, Italy, Aug./Sep. 2011, pp. 656–661.

[20] H. Vorobieva, S. Glaser, N. Minoiu-Enache, and S. Mammar, "Geometric path planning for automatic parallel parking in tiny spots," in *Proc. 13th IFAC Symp. Control Transp. Syst.*, Sofia, Bulgaria, Sep. 2012, pp. 36–42.

[21] H. Vorobieva, N. Minoiu-Enache, S. Glaser, and S. Mammar, "Geometric continuous-curvature path planning for automatic parallel parking," in *Proc. 10th IEEE Int. Conf. Netw., Sens. Control*, Evry, France, Apr. 2013, pp. 418–423.

[22] H. Vorobieva, S. Glaser, N. Minoiu-Enache, and S. Mammar, "Automatic parallel parking with geometric continuous-curvature path planning," in *Proc. IEEE Int. Symp. Intell. Veh.*, Dearborn, Michigan, USA, Jun. 2014, pp. 465–471.

[23] T. Fraichard and P. Garnier, "Fuzzy control to drive car-like vehicles," *Robot. Auton. Syst.*, vol. 34, no. 1, pp. 1–22, Jan. 2001.

[24] Y. Nakada, "Development of a parking assist system and corresponding autonomous driving in a parking lot," in *Proc. 2nd Int. Symp. Future Active Safety Technol. toward zero-traffic-accident*, Nagoya, Japan, Sep. 2013, pp. 1–8.

[25] K. Sung, J. Choi, and D. Kwak, "Vehicle control system for automatic valet parking with infrastructure sensors," in *Proc. IEEE Int. Conf. Consum. Electron.*, Las Vegas, NV, USA, Jan. 2011, pp. 567–568.

[26] D. Lyon, "A min-time analysis of three trajectories with curvature and nonholonomic constraints using a parallel parking criterion," *JSME Int. J. Ser. C*, vol. 46, no. 4, pp. 1523–1530, 2003.

[27] K. Komoriya and K. Tanie, "Trajectory design and control of a wheel-type mobile robot using b-spline curve," in *Proc. IEEE-RSJ Int. Conf. Intell. Robots Syst.*, Tsukuba, Japan, Sep. 1989, pp. 398–405.

[28] W. L. Nelson, "Continuous-curvature paths for autonomous vehicles," in *Proc. IEEE Int. Conf. Robot. Autom.*, Scottsdale, AZ, May 1989, pp. 1260–1264.

[29] A. Takahashi, T. Hongo, and Y. Ninomiya, "Local path planning and control for agv in positioning," in *Proc. IEEE-RSJ Int. Conf. Intell. Robots Syst.*, Tsukuba, Japan, Sep. 1989, pp. 392–397.

[30] R. Liscano and D. Green, "Design and implementation of a trajectory generator for an indoor mobile robot," in *Proc. IEEE-RSJ Int. Conf. Intell. Robots Syst.*, Tsukuba, Japan, Sep. 1989, pp. 380–385.

[31] Y. Kanayama and B. I. Hartman, "Smooth local path planning for autonomous vehicles," in *Proc. IEEE Int. Conf. Robot. Autom.*, Scottsdale, AZ, USA, May 1989, pp. 1265–1270.

[32] A. Piazzi and C. G. L. Bianco, "Quintic G ^{2}-splines for trajectory planning of autonomous vehicles," in *Proc. IEEE Intell. Veh. Symp.*, Dearborn, MI, USA, Oct. 2000, pp. 198–203.

[33] A. Scheuer and C. Laugier, "Planning sub-optimal and continuous-curvature paths for car-like robots," in *Proc. IEEE-RSJ Int. Conf. Intell. Robots Syst.*, Victoria, BC, Canada, Oct. 1998, pp. 25–31.

[34] Z. Liang, G. Zheng, and J. Li, "Automatic parking path optimization based on bezier curve fitting," in *Proc. IEEE Int. Conf. Autom. Logist.*, Zhengzhou, China, Aug. 2012, pp. 583–587.

[35] A. Scheuer and T. Fraichard, "Continuous- curvature path planning for car-like vehicles," in *Proc. IEEE-RSJ Int. Conf. Intell. Robots Syst.*, Grenoble, France, Sep. 1997, pp. 997–1003.

[36] T. Fraichard and A. Scheuer, "From Reeds and Shepp's to continuous-curvature paths," *IEEE Trans. Robot.*, vol. 20, no. 6, pp. 1025–1035, Dec. 2004.

[37] J.-D. Boissonnat, A. Cerezo, and J. Leblond, "A note on shortest paths in the plane subject to a constraint on the derivative of the curvature," Inst. Nat. de Recherche en Informatique et en Automatique, Paris, France, Tech. Rep. Res. Rep. 2160, Jan. 1994.

[38] *Dimensions des constructions—Parcs de stationnement usage privatif—Dimensions minimales des emplacements et des voies*, AFNOR French standard, Rev. NF P91-120, Apr. 1996.

[39] P. Bonnifait, P. Bouron, P. Crubillé, and D. Meizel, "Data fusion of four abs sensors and gps for an enhanced localization of car-like vehicles," in *Proc. IEEE Int. Conf Robot. Autom.*, Seoul, Korea, May 2001, pp. 1597–1602.

Hélène Vorobieva received the Dipl.-Ing. degree from Superior National School of Advanced Techniques (ENSTA ParisTech), Paris, France, in 2011 and the M.S. degree in advanced systems and robotics from University Pierre et Marie Curie, Paris, France, in 2011. She is currently working toward the Ph.D. degree in automatic control with University of Évry Val d'Essonne, Évry, France.

She has a CIFRE Ph.D. employment contract with Renault SAS, Guyancourt, France, in collaboration with Laboratoire sur les Interactions Véhicules-Infrastructure-Conducteurs (LIVIC), Institut Français des Sciences et Technologies des Transports, de l'Aménagement et des Réseaux (IFSTTAR), Versailles, France. Her research interests include automatic parking maneuvers.

Sébastien Glaser received the Dipl.-Ing. degree from National School of State Public Works (ENTPE), Vaulx en Velin, France, in 2000; the M.S. degree in image analysis and synthesis from Jean Monnet University, Saint-Étienne, France; and the Ph.D. degree in automatic control, with an emphasis on the vehicle dynamic analysis, and the Habilitation to Direct Research degree from University of Évry Val d'Essonne, Évry, France, in 2004 and 2010, respectively.

Since 2004 he has been a Researcher with Laboratoire sur les Interactions Véhicules-Infrastructure-Conducteurs, Institut Français des Sciences et Technologies des Transports, de l'Aménagement et des Réseaux, Versailles, France. Since 2009 he has led a research team on risk analysis, decision making and control. He has been involved in several European Union initiatives (e.g., eFuture and HAVEit) and has led a French initiative on low-speed automation (ANR-ABV). His research interests include driving-assistance design and driver studies.

Nicoleta Minoiu-Enache received the M.S. degree in electrical engineering and business administration from Technische Universitat Darmstadt, Darmstadt, Germany in 2004; the M.S. degree in control and signal processing from Université Paris-Sud, Orsay, France, in 2005; and the Ph.D. degree in automatic control from University of Évry Val d'Essonne, Évry, France, in 2008.

She is with Renault SAS, Guyancourt, France, as a Research and Development Engineer in the area of advanced driver assistance systems and automatic control.

Dr. Minoiu-Enache received the Best Ph.D. Thesis Award in Automatic Control from Groupe de Recherche Modèlisation, Analyse et Conduite de Systémes Dynamiques GdR MACS, France, in 2009 and the Excellence Award for the Master Thesis from the SEW-EURODRIVE Foundation, Germany, in 2005.

Saïd Mammar (SM'11) received the Dipl.-Ing. degree from École Supérieure d'Électricité, Gif-sur-Yvette, France, in 1989; the Ph.D. degree in automatic control from University Paris XI-Supelec, Orsay, France, in 1992; and the Habilitation to Direct Research degree from University of Évry Val d'Essonne, Évry, France, in 2001.

From 1992 to 1994 he held a research position with the French National Institute on Transportation Research and Safety, Versailles, France, where he was involved in research on traffic network control. Since 1994 he has been with University of Évry Val d'Essonne, first as an Assistant Professor (1994–2002) and currently as a Professor. From 2006 to September 2009 he was a Scientific and University Attachè with the French Embassy, Hague, The Netherlands. Since January 2010 he has been the Head of the Laboratoire Informatique, Biologie Intégrative et Systèmes Complexes, University of Évry Val d'Essonne. His research interests include robust control, vehicle longitudinal and lateral control for driving assistance, and intelligent transportation systems.